IEEE Access
Multidisciplinary | Rapid Review | Open Access Journal

Received October 26, 2020, accepted November 13, 2020, date of publication November 24, 2020,
date of current version December 9, 2020.

Digital Object Identifier 10.1109/ACCESS.2020.3039983

Joint Torque Closed-Loop Estimation Using NARX Neural Network Based on sEMG Signals

YURONG LI, WENXIN CHEN, HAO YANG, JIXIANG LI, AND NAN ZHENG
College of Electrical Engineering and Automation, Fuzhou University, Fuzhou 350108, China
Fujian Key Laboratory of Medical Instrumentation and Pharmaceutical Technology, Fuzhou University, Fuzhou 350108, China

Corresponding author: Yurong Li (liyurong@fzu.edu.cn)

This work was supported in part by the National Natural Science Foundation of China under Grant 61773124, and in part by the Fujian Province Nature Science Foundation of China under Grant 2019J01544.

ABSTRACT Joint torque estimation is of great significance for the research and clinical application of intelligent rehabilitation technology. This paper proposes a closed-loop model for joint torque estimation based on surface electromyography (sEMG). Combined with the physiological characteristics of muscle activation, a nonlinear autoregressive with eXogenous inputs(NARX) neural network model for joint torque estimation based on sEMG signals is established. In order to solve the drift phenomenon of torque estimation, a state-space framework is constructed by regarding NARX neural network based torque estimation model as state model and developing a measurement model by the easily measured joint angle signals. With the built state-space model, the extended Kalman filter (EKF) is used to realize the closed-loop filtering of the estimated torque. In order to test the accuracy of the proposed closed-loop joint torque estimation, 8 volunteers were recruited to perform elbow joint isotonic motion experiments under four kinds of loads. The test results show that the average normalized root mean square error (NRMSE) between the estimated values of closed-loop model and measurement values of all subjects under load-dependent, multi-load and load-independent tests are 0.1080±0.0411, 0.1326±0.0494 and 0.1674±0.0661 respectively, which is significant better than the results of the open-loop model (0.2694±0.1584 ($p < 10^{-6}$), 0.2499±0.1326 ($p < 10^{-6}$) and 0.3435±0.2061 ($p < 10^{-4}$)). The presented closed-loop model combines offline modeling and online filtering to achieve online estimation of joint torque, which ameliorates the problem that the estimated torque in the open-loop model deviates greatly from the actual values and improves the accuracy of joint torque estimation.

INDEX TERMS sEMG, neural network, NARX, EKF.

I. INTRODUCTION

In recent years, the prevalence of paralysis caused by spinal cord injury and stroke have been increasing significantly. According to the heart disease and stroke statistics report from the American Heart Association, the stroke prevalence of adult in the United States is 2.9%, and it is estimated that by 2030, more than 3.4 million US adults over the age of 18 will have had a stroke, a 20.5% increase in prevalence from 2012 [1]. Stroke and spinal cord injury can easily lead to tissue damage, and different degrees of tissue damage at different positions can cause different degrees of sports injuries, so most of these patients have varying degrees of decline in mobility. For such a large group of patients with motor dysfunction, it is very meaningful to help them recover and reconstruct their limb motor function. Human joint torque is one of the important parameters for quantitative analysis of human motion function, which is of great significance for realizing precise control of exoskeleton robots, quantitative evaluation of rehabilitation training [2]. The direct torque measurement system requires bulky equipment which requires complex mechanical structures and is limited by the environment. Therefore, estimation by other measurable parameters to achieve indirect measurement of joint torque has been widely studied. However, most of the existing researches on joint torque estimation are limited to isometric motion, which is a kind of static motion [3]. In fact, the torque estimation under motion state has much practical significance, for example, in the realization of motor control of rehabilitation robot.

The associate editor coordinating the review of this manuscript and approving it for publication was Hamid Mohammad-Sedighi.

Electromyography (EMG) signal represents the sum of subcutaneous motor action potentials generated by muscle contraction, which can represent neuromuscular activity [4]. It is an alternative to reflect the patient's voluntary effort. The training involving the patient's voluntary effort can improve the therapeutic effect [5]. The surface electromyography (sEMG) is a non-invasive EMG signal collected by surface electrodes, which has the advantage of being more accessible than electroencephalography (EEG) and less likely to impede the user's normal activities. The EMG signals can not only be used for motor pattern recognition [6], but also for the estimation of motor signals such as joint torque and angle. Research on wearable EMG devices have shown that between 150-300 ms of window length is required to avoid significant delays for the user. The appearance of the EMG signals is ahead of the actual joint motion [7], which is called electromechanical delay between the EMG signals and the actual joint motion. This feature is very important for the implementation of real-time control. So, the sEMG signals are usually used as intelligent human-machine interface to estimate torque or angle for the control of rehabilitation robot [8].

The joint torque estimation model based on EMG signals mainly has two model structures, namely, the mechanism model based on neurophysiology, and the data-driven black-box model. The mechanism model uses EMG signals as the control signal, builds a model according to the physiological structure of the human body, and outputs joint torque or joint motion [9]. Among these model, the Hill-type muscle model is the most commonly used one. The mechanism model driven by EMG signals usually consists of muscle activation model, Hill-type muscle contraction dynamics and joint dynamics [10], [11]. Meyer *et al.* developed a novel EMG-driven modeling method based on the Hill-type model that automatically adjusts surrogate representations of the patient's musculoskeletal geometry, which improved the accuracy of walking joint torque estimation compared to results from previous EMG-driven studies [12]. The model structure based on the Hill-type mechanism model has shown its excellence when it comes to complex movements involving multiple joints and is a hot topic of research in the field of biomechanics. However, the model is very complex and involves a large number of unknown physiological parameters, making the analysis and application of the model very difficult.

In contrast to the development of complex physiological models, in the data-driven black-box model approach, functional relationships are established without the need for explicit equations to model underlying neural activation and joint motion. Thus, in the black-box model, all intermediate functional relationships between the observed experimental variables are not explicitly modeled. However, they are contained within a macroscopic transfer function. The NARX model is an effective method for solving nonlinear sequence problems that better combines the nonlinear spatiotemporal correlation structure of natural human movement with muscle-driven control signals [13]. Dynamic recurrent neural networks based on the NARX model are widely used for joint angle estimation [14], decoding shoulder, elbow, and wrist movements [15], and prosthetic model control [16]. There are problems in the research of NARX model-based dynamic recurrent neural networks: firstly, the feature extraction of EMG signals by the existing models only considers the macroscopic characteristics of EMG signals, for instance, the amplitude characteristics such as mean absolute value, integrated EMG and root mean square, as well as waveform characteristics such as waveform length and zero crossing, without considering the microscopic physiological characteristics of muscle activation; secondly, the functional relationships obtained in specific conditions may not be applicable to the new conditions [17]. This is related to the fact that a single macroscopic nonlinear transfer function may not be sufficient to capture the complexity of the several intermediate nonlinear components that exist among the observables. EMG signals are typically non-stationary in real time [18], so the online application of the offline trained model may introduce estimation errors and even instability.

In this paper, considering the physiological characteristics of microscopic muscle activation, a second-order dynamic system was used to simulate the muscle activation dynamics, and then the muscle activation was used as the EMG signal feature as the input of the NARX neural network model. The NARX neural network simulated the process of muscle contraction dynamics and joint dynamics to generate the joint torque. Furthermore, in order to avoid the instability of the torque autoregressive signal in the NARX model, the torque signal was filtered to overcome the signal drift by forming a closed-loop model structure for joint torque estimation based on a nonlinear filtering algorithm with an easy-to-measure joint angle signal. Compared to the existing state of the art, the proposed method has the following advantages: (1) The physiological properties of muscle activation and the complex nonlinear mapping and learning capabilities of neural networks are combined to perform joint torque estimation based on sEMG signals; (2) We use easy-to-measure motion parameters to form a closed-loop model, filter the output torque of neural networks to improve the estimation accuracy of joint torque; (3) Only one pair of antagonistic muscle EMG signals are used to reduce the cost of EMG signal detection, which allows for online torque estimation of wearable devices.

II. MATERIALS AND METHODS

A. NARX NEURAL NETWORK TORQUE ESTIMATION MODEL BASED ON SEMG SIGNALS

1) MUSCLE ACTIVATION DYNAMICS

The sEMG signal is the sum of the action potentials recruited to the muscle by surface electrodes and is used to reflect the level of muscle activation. The sEMG signal can be considered as the characterization of neuromotor control commands and is widely used to analyze musculoskeletal models. In order to reflect the microscopic physiological characteristics and reflect the relationship between EMG signal, neural

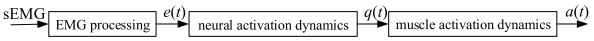

FIGURE 1. Muscle activation dynamics.

activation and muscle activation, this paper considered the physiological characteristics of microscopic muscle activation and established a muscle activation dynamics model to extract the EMG signal feature [19]. Muscle activation dynamics is mainly represented by the transformation process between EMG signal and muscle activation, as shown in Figure 1.

Raw sEMG signals was firstly high-pass filtered (4th order, cutoff frequency 20Hz) to eliminate low-frequency noise, then full-wave rectified and low-pass filtered (4th order, cutoff frequency 4Hz), and finally normalized to obtain the processed sEMG signal $e(t)$.

When a muscle fiber is activated by a single action potential, the muscle generated a twitch response. This response can be represented by a critically damped linear second-order differential system [20]. This type of response is the basis of different equations for determining the neural activation $q(t)$ based on the sEMG signal $e(t)$:

$$q(t) = K_1 \frac{de^2(t)}{dt^2} + K_2 \frac{de(t)}{dt} + K_3 e(t) \tag{1}$$

where K_1, K_2 and K_3, are the constants that define the dynamics of the second-order system.

Equation (1) is a continuous form of the second-order differential equation, however the data collected are discrete, resulting in discrete EMG signals time series. Thus, equation (1) is discretized to obtain a second-order discrete linear model [21], [22]:

$$q(t) = \alpha e(t-d) - \beta_1 q(t-1) - \beta_2 q(t-2) \tag{2}$$

where d is the electromechanical delay, α the gain coefficient, β_1 andβ_2 the recursive coefficients.

Equation (2) can be viewed as a recursive filter, where the current value of neural activation closely correlates with that of the approaching torque, consistent with the cumulative response of the muscular system. In order to ensure the stability of the second-order system, constraints are determined from the z transform of (2) as follows:

$$\begin{aligned} H(z) &= \frac{q(z)}{e(z)} = \frac{\alpha}{1+\beta_1 z^{-1}+\beta_2 z^{-2}} = \frac{\alpha}{(1+\gamma_1 z^{-1})(1+\gamma_2 z^{-1})} \\ \beta_1 &= \gamma_1 + \gamma_2 \\ \beta_2 &= \gamma_1 \times \gamma_2 \end{aligned} \tag{3}$$

Depending on the stability conditions of the system, the system parameters are constrained as shown in (4) [21], [22]:

$$|\gamma_1| < 1, |\gamma_2| < 1, \alpha - \beta_1 - \beta_2 = 1 \tag{4}$$

The value of γ_1 and γ_2 change the impulse response of the second-order filter. The recursive filter generates undamped response if both γ_1 and γ_2 are positive, and damped response if γ_1 and γ_2 are negative. The damped second-order response lengthens the EMG signal processing time, while the electromechanical delay improves the synchronization between activation and force generation, ameliorating the problem of asynchrony between muscle activation and muscle force.

It has been shown that EMG signals are not necessarily linearly correlated with muscle force [23], and (5) was chosen to describe the nonlinear relationship between neural activation and muscle activation:

$$a(t) = \frac{e^{Aq(t)} - 1}{e^A - 1} \tag{5}$$

where $a(t)$ is the muscle activation, $q(t)$ the neural activation, A the non-linear shape factor, constrained to -3<A<0.

2) NARX NEURAL NETWORK MODEL

Nonlinear Auto-Regressive with eXogenous inputs (NARX) model is an effective method for solving nonlinear sequence problems that accommodates nonlinear discrete time processes and noisy models [24], [25]. NARX model predicts the current value of a system output by using a nonlinear function f with previous inputs and outputs, and there are two forms of prediction using the NARX model [26]. One is a NARX model based on the actual values of output:

$$\hat{y}_k = f(u_k, u_{k-1} \ldots, u_{k-n_u}, y_{k-1}, y_{k-2}, \ldots, y_{k-n_y}) \tag{6}$$

The other is a NARX model based on the estimated values of output:

$$\hat{y}_k = f(u_k, u_{k-1} \ldots, u_{k-n_u}, \hat{y}_{k-1}, \hat{y}_{k-2}, \ldots, \hat{y}_{k-n_y}), \tag{7}$$

where $f(\cdot)$ is the nonlinear function between the input u_k and the estimated value $\hat{y}_k$ of the actual output y_k, k represents kth time step, n_u and n_y are the maximum lags for model input and output, respectively.

The multi-layer feedforward network has a highly nonlinear mapping capability, so in this paper it is used to implement the NARX model and form a dynamic recurrent neural network for joint torque estimation. In this paper, a single hidden layer feedforward neural network is adopted, with the $tansig(\cdot)$ as the activation function at the hidden layer and a linear activation function at the output layer. The function relationship between input and output of the single hidden layer network is given as:

$$y = \sum_{j=1}^{n} (\delta_j tansig(\sum_{i=1}^{m} (\omega_{ij} u_i + \theta_i))) + \vartheta \tag{8}$$

where u_i and θ_i represent the input and bias of the ith input unit respecitively, ω_{ij} represents the weight of the ith unit of the input layer to the jth unit of the hidden layer, δ_j represents the weight of the jth unit of the hidden layer to the output unit, ϑ represents the bias of the output layer, $i = 1, 2, \ldots, m$, $j = 1, 2, \ldots, n$, m is the number of input units, and n is the number of hidden layer units.

$tansig(\cdot)$ is the activation function of the hidden layer:

$$tansig\,(x) = tanh(x) = \frac{e^x - e^{-x}}{e^x + e^{-x}} \tag{9}$$

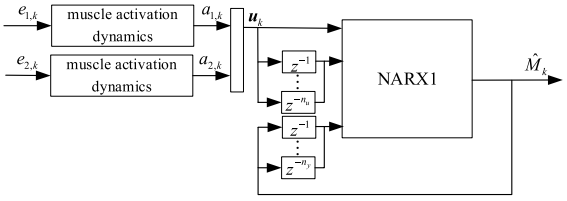

FIGURE 2. NARX neural network based torque estimation model.

To speed up the calculation, (9) is equated to

$$tansig\,(x) = \frac{2}{1+e^{-2x}} - 1. \tag{10}$$

Substituting (6) and (7) into (8) respectively, we get two implementations of the NARX dynamic recurrent neural network as:

$$\hat{y}_k = \sum_{j=1}^{n}(\delta_j tansig(\sum_{i=1}^{n_u+1}(\omega_{ij}u_{k-i+1} + \theta_i) + \sum_{i=n_u+2}^{n_u+n_y+1}(\omega_{ij}y_{k-i+n_u+1} + \theta_i)))+\vartheta \tag{11}$$

$$\hat{y}_k = \sum_{j=1}^{n}(\delta_j tansig(\sum_{i=1}^{n_u+1}(\omega_{ij}u_{k-i+1} + \theta_i) + \sum_{i=n_u+2}^{n_u+n_y+1}(\omega_{ij}\hat{y}_{k-i+n_u+1} + \theta_i)))+\vartheta \tag{12}$$

Equation (11) is used to realize one-step ahead prediction in case of known actual output. Equation (12) is used when the actual output is unknown so as to realize estimation. The latter relies on autoregression of the estimated output, easily leading to some problems such as drift and instability of the estimated results. And its estimation accuracy is low.

3) NARX NEURAL NETWORK BASED TORQUE ESTIMATION MODEL

In this paper, a NARX neural network based torque estimation model was developed using sEMG signals from a pair of antagonist muscles (biceps brachii and triceps brachii) that control elbow joint motion, as shown in Figure 2. The $e_{1,k}$ and $e_{2,k}$ were the processed sEMG signals of the biceps brachii and triceps brachii, and the muscle activation $a_{1,k}$ and $a_{2,k}$ were then calculated through the muscle activation dynamics respectively to form the input $\boldsymbol{u}_k = \left[a_{1,k}, a_{2,k}\right]^T$. The input and output of NARX dynamic recurrent neural network was $\boldsymbol{u}_k$ and joint torque, where k represents kth time step, $\hat{M}_k$ was joint torque estimation, n_u and n_y were the maximum lags for model input and output of the model respectively.

Due to the bulky size of the direct torque measurement equipment, joint torque estimation by (12) is more meaningful. It allows for online real-time torque estimation. Therefore, in this paper, the open-loop model for joint torque estimation was established by NARX dynamic recurrent neural network based on the estimated values, denoted as NARX1 in Figure 2. The output was estimated joint torque $\hat{M}_k$ given as:

$$\hat{M}_k = \sum_{j=1}^{n_1}(\delta_{1,j} tansig(\sum_{i=1}^{n_{u1}+1}(\omega_{1,ij}\boldsymbol{u}_{k-i+1} + \theta_{1,i}) + \sum_{i=n_{u1}+2}^{n_{u1}+n_{y1}+1}(\omega_{1,ij}\hat{M}_{k-i+n_{u1}+1} + \theta_{1,i})))+\vartheta_1 \tag{13}$$

where the subscript 1 of $\theta_{1,i}$, $\omega_{1,ij}$, $\delta_{1,j}$ and ϑ_1 was the parameter that represented NARX1, which was distinguished from other neural network models later on, n_{u1} and n_{y1} were the order of input and output, respectively. In order to improve the computational efficiency, the Levenberg-Marquardt algorithm was used to train the open-loop model. The effect of the number of hidden layer units on the estimation accuracy was pre-tested and found that increasing the number of hidden layer units within a certain range can improve the estimation accuracy, while continuing to increase the number of hidden layer units does not improve the estimation accuracy significantly, or even decreases it. Considering the model accuracy and the complexity of the model, the number of hidden layer units was determined to be $n_1 = 5$.

B. CLOSED-LOOP MODEL FOR TORQUE ESTIMATION

The neural network model suffers from the problem that the functional relationships obtained in specific conditions may not be applicable to new conditions, and the NARX dynamic recurrent neural network model based on output estimation suffers from the problem of unstable estimation results and the influence of noise. To solve these problem, this paper established a closed-loop model for joint torque estimation, as shown in Figure 3.

1) STATE SPACE MODEL

Since the joint angle can be easily measured by the inertial measurement unit, this paper established another NARX dynamic recurrent neural network model NARX2, which characterized the relationship between torque and angle based on the actual measurements of the joint angle, as the measurement model:

$$\hat{y}_k = \sum_{j=1}^{n_2}(\delta_{2,j} tansig(\sum_{i=1}^{n_{u2}+1}(\omega_{2,ij}M_{k-i+1} + \theta_{2,i}) + \sum_{i=n_{u2}+2}^{n_{u2}+n_{y2}+1}(\omega_{2,ij}y_{k-i+n_{u2}+1} + \theta_{2,i})))+\vartheta_2 \tag{14}$$

where the subscript 2 of $\theta_{2,i}$, $\omega_{2,ij}$, $\delta_{2,j}$ and ϑ_2 was the parameter that represented NARX2, n_{u2} and n_{y2} were the maximum lags for model input and output, respectively, and the number of hidden layer units $n_2 = 5$, output y_k was the joint angle.

Defining state vector to be joint torque vector. We assumed the process noise and the measurement noise to be the Gaussian white noise. State space model was developed for torque estimation based on state equation (13) and measurement

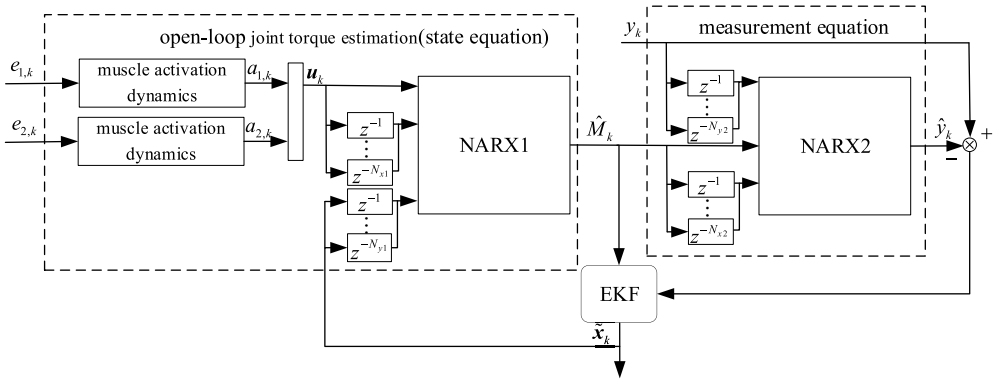

FIGURE 3. Closed-loop joint torque estimation model.

equation (14), as in (15) and (16), as shown at the bottom of the page.

In equation (15) and (16), $N = max(N_{y1}, N_{x2})$, N_{x1} and N_{y1} were the maximum lags for $\boldsymbol{u}_k$ and $\boldsymbol{x}_k$ of the state model, N_{x2} and N_{y2} were the maximum lags for $\boldsymbol{x}_k$ and y_k of the output model.

2) TORQUE ESTIMATION BASED ON EXTENDED KALMAN FILTER

Extended Kalman filter (EKF) is widely used for online state estimation of discrete-time nonlinear systems because of its advantages in training efficiency and accuracy [27], so in this paper, EKF is utilized for closed-loop estimation of joint torque.

Muscle activation was first calculated using the sEMG signals, and then muscle activation and normalized joint torque and joint angle measurements were used to train NARX1 and NARX2 offline using the Levenberg-Marquardt algorithm, respectively.

The trained input and output models were then used to establish state space model, and a closed-loop model structure for joint torque estimation was formed based on EKF to perform state filtering.

Compute the Jacobian of the state and measurement function:

$$\boldsymbol{G}_k = \frac{\delta \boldsymbol{g}(\boldsymbol{x}_k)}{\delta \boldsymbol{x}_k} \tag{17}$$

$$\boldsymbol{H}_k = \frac{\delta h(\boldsymbol{x}_k)}{\delta \boldsymbol{x}_k} \tag{18}$$

The recursive estimation of the state space model by EKF consists of the following two stages [27]:

Time update (predict)

$$\hat{\boldsymbol{x}}_k = \boldsymbol{g}(\boldsymbol{x}_{k-1}, \boldsymbol{u}_k) \tag{19}$$
$$\boldsymbol{P}_k^- = \boldsymbol{G}_k \boldsymbol{P}_{k-1} \boldsymbol{G}_k{}^T + \boldsymbol{Q} \tag{20}$$
$$\hat{y}_k = h(\hat{\boldsymbol{x}}_k, \boldsymbol{u}_k) \tag{21}$$

Measurement update (correct)

$$\boldsymbol{K}_k = \boldsymbol{P}_k^- \boldsymbol{H}_k^T (\boldsymbol{H}_k \boldsymbol{P}_k^- \boldsymbol{H}_k^T + \boldsymbol{R})^{-1} \tag{22}$$
$$\tilde{\boldsymbol{x}}_k = \hat{\boldsymbol{x}}_k + \boldsymbol{K}_k (y_k - \hat{y}_k) \tag{23}$$
$$\boldsymbol{P}_k = (\boldsymbol{I} - \boldsymbol{K}_k \boldsymbol{H}_k) \boldsymbol{P}_k^- \tag{24}$$

where $\tilde{\boldsymbol{x}}_k$ represented the filtered value of state vector, $\tilde{M}_k = \tilde{x}_{1,k}$ was the closed-loop estimation of joint torque, $\boldsymbol{Q}$ the process noise covariance, $\boldsymbol{R}$ the measurement noise covariance, $\boldsymbol{P}_k$ the estimation error covariance matrix, $\boldsymbol{K}_k$ the Kalman gain.

C. PERFORMANCE EVALUATION AND STATISTICAL ANALYSIS

Normalized root mean square error (NRMSE) and correlation coefficient (CC) were taken as indicators to evaluate the performance of joint torque estimation, as shown

$$\begin{aligned} \boldsymbol{x}_k &= \boldsymbol{g}(\boldsymbol{x}_{k-1}, \boldsymbol{u}_k, \boldsymbol{u}_{k-1}, \ldots, \boldsymbol{u}_{k-N_{x1}}) + \boldsymbol{\omega}_k \\ y_k &= h(\boldsymbol{x}_k, y_{k-1}, y_{k-2}, \ldots, y_{k-N_{y2}}) + \nu_k \end{aligned} \tag{15}$$

$$\boldsymbol{g}(\cdot) = \begin{pmatrix} \sum_{j=1}^{n_1} (\delta_{1,j} tansig(\sum_{i=1}^{N_{x1}+1} (\omega_{1,ij} \boldsymbol{u}_{k-i+1} + \theta_{1,i}) + \sum_{i=N_{x1}+2}^{N_{x1}+N_{y1}+1} (\omega_{1,ij} \boldsymbol{x}_{i-N_{x1}-1} + \theta_{1,i}))) + \vartheta_1 \\ x_{1,k} \\ \vdots \\ x_{N,k} \end{pmatrix}$$

$$h(\cdot) = \sum_{j=1}^{n_2} (\delta_{2,j} tansig(\sum_{i=1}^{N_{x2}+1} (\omega_{2,ij} \boldsymbol{x}_{i,k} + \theta_{2,i}) + \sum_{i=N_{x2}+2}^{N_{x2}+N_{y2}+1} (\omega_{2,ij} y_{k-i+N_{x2}+1} + \theta_{2,i}))) + \vartheta_2 \tag{16}$$

TABLE 1. Subject Information.

Subjects	Gender	Age (years)	Height (cm)	Weight (kg)
S1	male	25	167	50
S2	male	25	168	60
S3	male	23	168	70
S4	male	22	177	67
S5	female	21	160	40
S6	male	27	173	55
S7	male	24	170	56
S8	female	46	172	65

in (25) and (26):

$$NRMSE = \frac{1}{M_{real}^{\max}}\sqrt{\frac{1}{num}\sum_{i=1}^{num}(M_{est}-M_{real})^2} \quad (25)$$

$$CC = \frac{cov(M_{est}, M_{real})}{\sigma_{M_{est}} \cdot \sigma_{M_{real}}} \quad (26)$$

where num was the number of test samples, M_{est} the estimated values of joint torque, M_{real} the measurements of joint torque, $M_{real}^{\max}$ the maximum measurements of joint torque.

One-way analysis of variance (ANOVA) was conducted to assess the statistical difference of estimation errors obtained by different models [28]. The level of statistical significance was set to $p < 0.05$.

III. EXPERIMENTS AND RESULTS

A. EXPERIMENTAL SETUP AND DATA ACQUISITION

In this section, experiment was conducted to validate the proposed method. Eight healthy subjects volunteered to participate in the experiment (right-handed, age: 26.62 ± 7.53 years; height: 169.37 ± 4.68 cm; weight: 57.87 ± 9.21 kg, two of whom were female). The healthy subjects had no history of neuromuscular disorders, pain, or experience with regular upper extremity training. Subject information is shown in Table 1.

The sEMG signal was acquired using Delsys Trigno Lab Wireless Acquisition System (Trigno Wireless System, Delsys Inc., USA) with a sampling frequency of 2000 Hz, a bandwidth of 20-500 Hz, and a high common mode rejection ratio (CMRR > 80dB). The Goniometer sensor SG 150 (Biometrics Ltd., England) acquired angle signals at 148 Hz with an adapter for data transmission to the Trigno Wireless System. Torque measurement acquisition was performed using a Biodex Pro4 system (Biodex Medical Systems Inc., NY, USA). Using a custom synchronization system, the torque and sEMG signals were acquired synchronously via an adapter so that the torque signal acquisition frequency was the same as the sEMG signal acquisition frequency. Finally, all signals were resampled so that the frequency was the same as the angle signal frequency. The experimental environment is shown in Figure 4.

The sEMG signals, angle signals and torque signals of the isotonic motion of the elbow joint under different loads were collected for subsequent analysis. Isotonic motion is exercise when a contracting muscle shortens against a constant load. When the torque produced by the subject's muscle

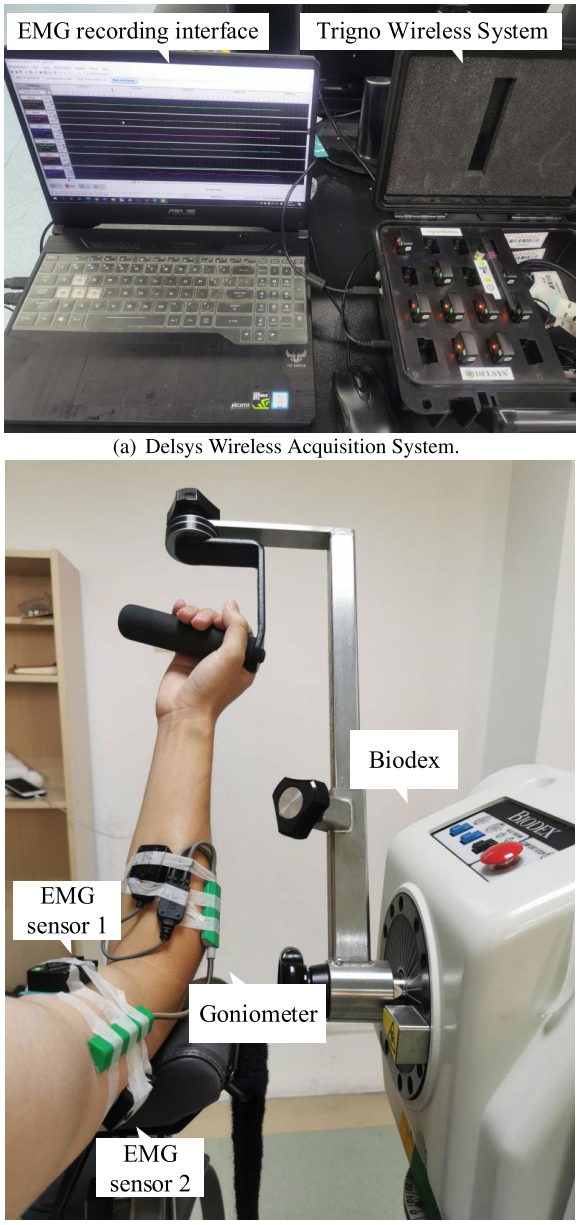

(a) Delsys Wireless Acquisition System.

(b) Illustration of Sensor Wearing Position.

FIGURE 4. Experimental environment set-up.

contraction is greater than the load provided by the device, the trainer's joint accelerates; when the torque produced by the muscle contraction is less than the load provided by the device, the trainer's joint decelerates. In this experiment, the subject was asked to perform isometric motion of the elbow joint in the sagittal plane, and the wireless EMG signal sensors were placed on the muscle belly of the biceps and triceps respectively (EMG sensor 1 and EMG sensor 2), and the goniometer was placed at the elbow joint. The isometric motion was set up with loads of 2 N·m, 4 N·m, 6 N·m and 8 N·m for 5 cycles of isometric exercise under each load.

Using the muscle activation dynamics from Section II-A1 to achieve feature extraction of sEMG signals, the raw

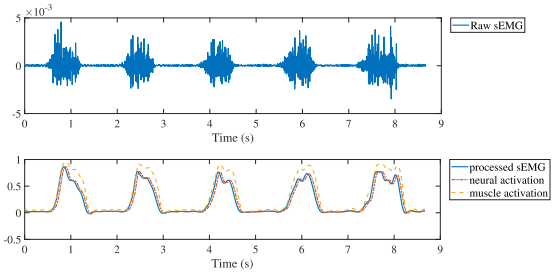

FIGURE 5. Feature extraction of sEMG signals.

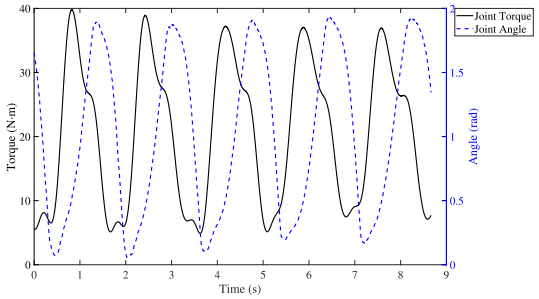

FIGURE 6. Joint angle and torque signals.

sEMGs, processed sEMG signals, neural activation and muscle activation of subject 4 (S4) for five cycles of isometric motion at a load of 6 N·m are shown in Figure 5, and joint angle and torque signals are shown in Figure 6.

B. DATA ALLOCATION STRATEGY

In order to investigate the influence of different loads of isometric motion on the joint torque estimation results, this paper analyzed the estimation results under three conditions: load-dependent, multi-load, and load-independent. Load-dependent took the first three cycles of each load as a training set, and the last two cycles at the corresponding load as test set; multi-load took the first three cycles of each load together as a training set, and the last two cycles of each load separately as a test set; the load-independent test took the last two cycles of one load in turn as test set, and the first three cycles of each unselected load together as training set.

C. ESTIMATION RESULTS

First, the model was trained offline according to the data allocation strategy. NARX1 was a NARX dynamic recurrent neural network model based on estimated values. Its input was the muscle activation extracted from the sEMG signals of the biceps and triceps with maximum lags N_{x1}=2 for input, $\gamma_1=\gamma_2$=0.5, A=-2, and the output was the normalized joint torque with maximum lags N_{y1}=2 for output. NARX2 was another NARX dynamic recurrent neural network model based on measurement values with maximum lags N_{x2}=2 for input and N_{y2}=2 for output. The input was the normalized joint torque and the output was the normalized joint angle.

The trained model was then used to perform joint torque estimation. In order to verify the improvement of closed-loop model, we tested the joint estimation results of the NARX neural network based torque estimation model (denoted as NN) and the closed-loop model (denoted as EKFSS).

We tested the joint torque estimation from all subjects under the three conditions of load-dependent, multi-load, and load-independent, and the results for S4 are shown in Figure 7, 8, and 9, where 'EKFSS' was the joint torque estimation from the closed-loop model, 'NN' was the joint torque estimation based on the NARX neural network model, and 'true' was the measurements of the joint torque. From Figure 7 to 9, it can be concluded that the estimation of joint torque based on the NARX neural network model has a large error. After adding the EKF filtering algorithm, the error of closed-loop estimation using the state space model is significantly reduced, and the estimated joint torque can approximate to the 'true' values overall.

The mean value of NRMSE and CC under different loads for the three conditions are shown in Figure 10 and Figure 11. The joint torque estimation of the closed-loop state space model with EKF is significantly better than the joint torque estimation based on the NARX neural network model. The error between the measurement values and the closed-loop joint torque estimation is relatively small, and the closed-loop estimation of the joint moment is strongly correlated with the measurement values.

Table 2 and Table 3 show the NRMSE and CC between the estimated joint torque of different models and the measurements ('true' values) of all subjects (mean ± standard deviation (std)). The mean CC between the EKFSS and 'true' values of all subjects were significantly larger than NN and the mean NRMSE were significantly smaller. The mean NRMSE of NN under load-dependent, multi-load and load-independent of all subjects are 0.2694±0.1584, 0.2499±0.1326 and 0.3435±0.2061, respectively, and EKFSS are 0.1080±0.0411, 0.1326±0.0494 and 0.1674± 0.0661, respectively. ANOVA was used to evaluate NRMSE of NN and EKFSS, showing significant differences ($p < 10^{-6}$, $p < 10^{-6}$ and $p < 10^{-4}$). It can also be found that the joint torque estimation results of the closed-loop model for the three cases are optimal for load-dependent estimation, with the smallest NRMSE (0.1080), followed by multi-load (0.1326), and worst for load-independent (0.1674). The variability of joint motion with different loads can affect the estimation of the model, and the experimental results also demonstrated that the load-dependent results were optimal and the load-independent results were the worst.

In this paper, in order to achieve joint torque estimation without torque measurement values, the estimation of NARX neural network model was based on estimated values. Thus, the error of joint toque estimation results has a great influence on the subsequent estimation results, which leads to the

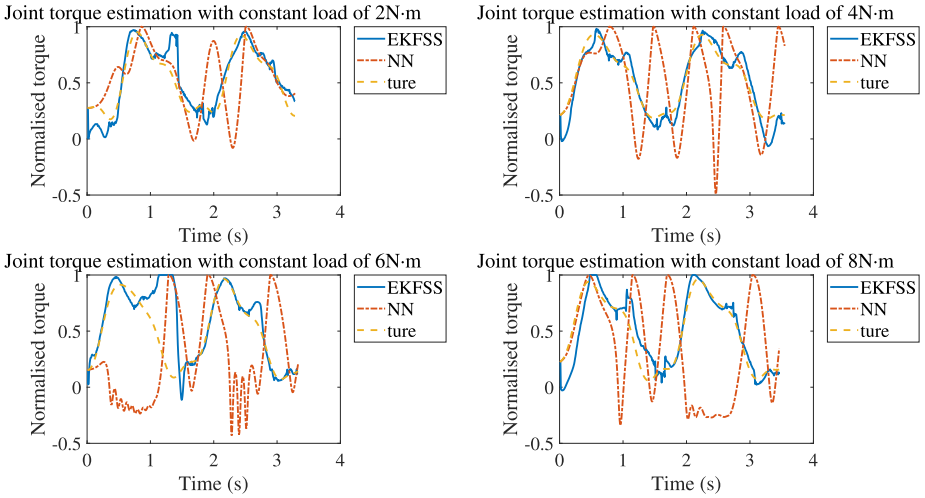

FIGURE 7. Joint torque estimation under load-dependent of S4.

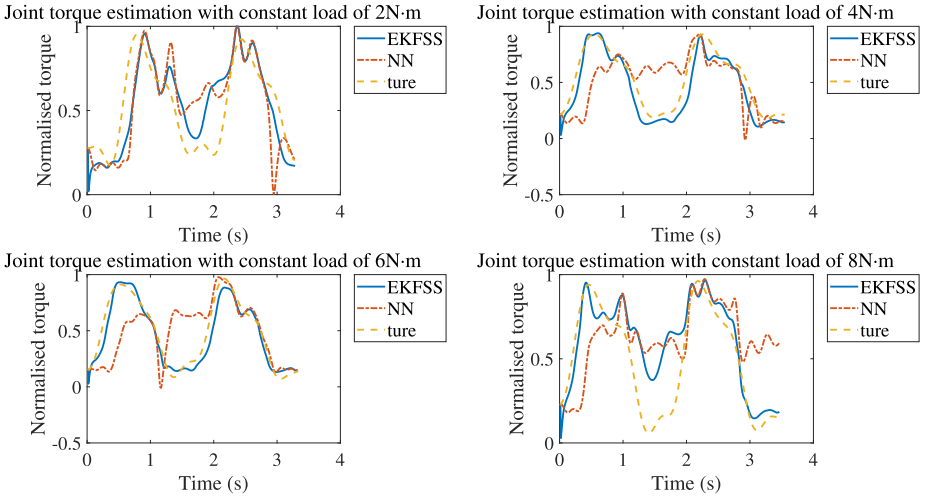

FIGURE 8. Joint torque estimation under multi-load of S4.

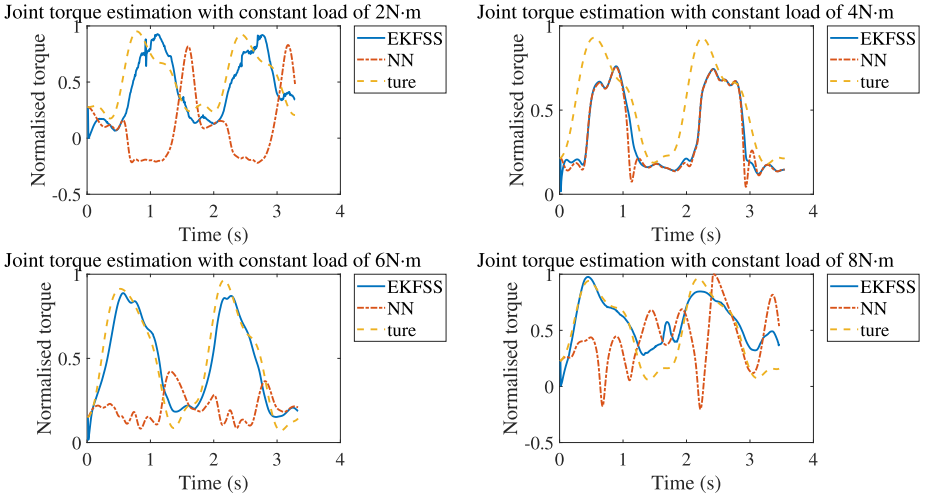

FIGURE 9. Joint torque estimation under load-independent of S4.

unstable performance of the torque estimation, with relatively large error and low correlation. Using joint angle signals to establish a closed-loop estimation model for joint torque improves the accuracy of joint torque estimation.

TABLE 2. NRMSE between the estimated joint torque of different models and the measurements ('true' values) of all subjects (mean ± std).

		2N.m	4N.m	6N.m	8N.m
load-dependent	NN	0.2129±0.1380	0.2181±0.0939	0.2874±0.1932	0.3591±0.1447
	EKFSS	0.0935±0.0176	0.0999±0.0189	0.1051±0.0654	0.1336±0.0298
multi-load	NN	0.2491±0.1151	0.2506±0.0949	0.2715±0.1023	0.2284±0.0701
	EKFSS	0.1486±0.0525	0.1042±0.0249	0.1166±0.0505	0.1610±0.0414
load-independent	NN	0.4181±0.2572	0.3624±0.2374	0.2783±0.1223	0.3150±0.1466
	EKFSS	0.1821±0.0682	0.1456±0.0532	0.1714±0.0680	0.1708±0.0684

TABLE 3. CC between the estimated joint torque of different models and the measurements ('true' values) of all subjects (mean ± std).

		2N.m	4N.m	6N.m	8N.m
load-dependent	NN	0.6108±0.2541	0.5648±0.3420	0.4634±0.4891	0.4381±0.3698
	EKFSS	0.8926±0.0990	0.9257±0.0562	0.9233±0.0930	0.9124±0.0532
multi-load	NN	0.5788±0.2510	0.6358±0.2492	0.5887±0.2994	0.6908±0.2586
	EKFSS	0.8457±0.0842	0.9254±0.0775	0.9258±0.0794	0.8862±0.0847
load-independent	NN	0.3040±0.5503	0.5945±0.2462	0.4689±0.5083	0.5732±0.3147
	EKFSS	0.7956±0.1430	0.8743±0.0602	0.8541±0.1261	0.8838±0.0632

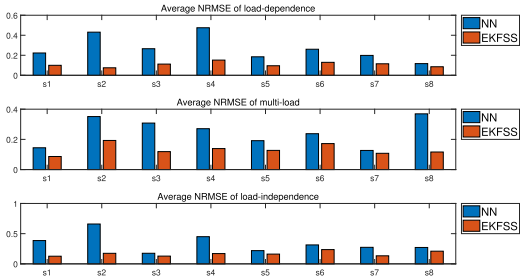

FIGURE 10. Average NRMSE for estimation of joint torque under different loads.

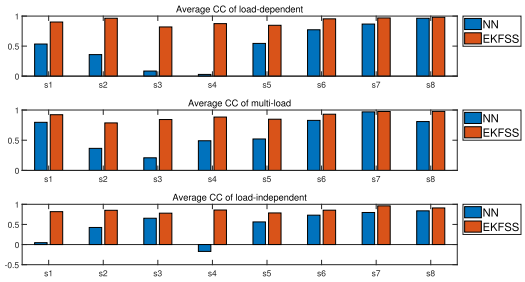

FIGURE 11. Average CC for estimation of joint torque under different loads.

IV. DISCUSSION AND CONCLUSION

EMG signals are widely used in scientific research related to the development of intelligent rehabilitation technology and equipment [29]. The EMG signal contains a wealth of motion information that precedes actual joint motion and is often used as a control signal to predict joint motion. Previous studies have focused on feature extraction and classification of EMG signals for identifying movement patterns [30], gait analysis [31], and joint angle estimation [32], [33]. Joint torque measurements are more complicated relative to joint angles due to the complexity of the human joint structure. The closed-loop model designed in this paper uses the EKF filtering algorithm to optimize the closed-loop model, improve the joint torque estimation results, and provide a new strategy for real-time joint torque estimation.

Taking the elbow joint as the research object, this paper designs a closed-loop model of joint torque estimation based on sEMG signals. A series of processing of the sEMG signals of the biceps and triceps were performed, and the muscle activation was obtained from the muscle activation dynamics. A torque estimation model was developed using a dynamic recurrent neural network based on the NARX model. To address the instability of the NARX neural network model and the influence of interference, a state-space closed-loop model with EKF algorithm for joint torque estimation was further designed. Finally, an isotonic motion experiment of elbow joint was designed to verify the actual estimation effect of the joint torque estimation model. The designed closed-loop model estimation improved the stability, and the NRMSE was significantly lower than that of the open-loop model. The proposed method combined offline modeling and online filtering to achieve online estimation of joint torque.

Although this article takes the elbow joint as the research object for model research and verification, the closed-loop model for torque estimation proposed in this paper is not limited to elbow joint torque estimation. In further study, the proposed torque estimation model can be applied to the torque estimation of other joints for related testing and validation.

REFERENCES

[1] E. J. Benjamin, P. Muntner, A. Alonso, M. S. Bittencourt, C. W. Callaway, A. P. Carson, A. M. Chamberlain, A. R. Chang, S. Cheng, and S. R. Das, "Heart disease and stroke statistics-2019 update a report from the American heart association," *Circulation*, vol. 139, no. 10, pp. 56–528, Jan. 2019.

[2] M. M. Ardestani, X. Zhang, L. Wang, Q. Lian, Y. Liu, J. He, D. Li, and Z. Jin, "Human lower extremity joint moment prediction: A wavelet neural network approach," *Expert Syst. Appl.*, vol. 41, no. 9, pp. 4422–4433, Jul. 2014.

[3] Q. Zhang, M. Hayashibe, and C. Azevedo-Coste, "Evoked electromyography-based closed-loop torque control in functional electrical stimulation," *IEEE Trans. Biomed. Eng.*, vol. 60, no. 8, pp. 2299–2307, Aug. 2013.

[4] U. Cote-Allard, C. L. Fall, A. Drouin, A. Campeau-Lecours, C. Gosselin, K. Glette, F. Laviolette, and B. Gosselin, "Deep learning for electromyographic hand gesture signal classification using transfer learning," *IEEE Trans. Neural Syst. Rehabil. Eng.*, vol. 27, no. 4, pp. 760–771, Apr. 2019.

[5] J.-I. Furukawa, T. Noda, T. Teramae, and J. Morimoto, "Human movement modeling to detect biosignal sensor failures for myoelectric assistive robot control," *IEEE Trans. Robot.*, vol. 33, no. 4, pp. 846–857, Aug. 2017.
[6] M. Gandolla, S. Ferrante, G. Ferrigno, D. Baldassini, F. Molteni, E. Guanziroli, M. C. Cottini, C. Seneci, and A. Pedrocchi, "Artificial neural network EMG classifier for functional hand grasp movements prediction," *J. Int. Med. Res.*, vol. 45, no. 6, pp. 1831–1847, Dec. 2017.
[7] D. M. Corcos, G. L. Gottlieb, M. L. Latash, G. L. Almeida, and G. C. Agarwal, "Electromechanical delay: An experimental artifact," *J. Electromyogr. Kinesiol.*, vol. 2, no. 2, pp. 59–68, Jan. 1992.
[8] J. A. Spanias, E. J. Perreault, and L. J. Hargrove, "Detection of and compensation for EMG disturbances for powered lower limb prosthesis control," *IEEE Trans. Neural Syst. Rehabil. Eng.*, vol. 24, no. 2, pp. 226–234, Feb. 2016.
[9] M. Sartori, M. Reggiani, D. Farina, and D. G. Lloyd, "Emg-driven forward-dynamic estimation of muscle force and joint moment about multiple degrees of freedom in the human lower extremity," *PLoS ONE*, vol. 7, no. 12, pp. 1–11, 2012.
[10] C. Fleischer and G. Hommel, "A human-exoskeleton interface utilizing electromyography," *IEEE Trans. Robot.*, vol. 24, no. 4, pp. 872–882, Aug. 2008.
[11] E. E. Cavallaro, J. Rosen, J. C. Perry, and S. Burns, "Real-time myoprocessors for a neural controlled powered exoskeleton arm," *IEEE Trans. Biomed. Eng.*, vol. 53, no. 11, pp. 2387–2396, Nov. 2006.
[12] A. J. Meyer, C. Patten, and B. J. Fregly, "Lower extremity emg-driven modeling of walking with automated adjustment of musculoskeletal geometry," *PLoS ONE*, vol. 12, no. 7, pp. 1–24, 2017.
[13] M. Xiloyannis, C. Gavriel, A. A. C. Thomik, and A. A. Faisal, "Gaussian process autoregression for simultaneous proportional multi-modal prosthetic control with natural hand kinematics," *IEEE Trans. Neural Syst. Rehabil. Eng.*, vol. 25, no. 10, pp. 1785–1801, Oct. 2017.
[14] R. Gupta, I. S. Dhindsa, and R. Agarwal, "Continuous angular position estimation of human ankle during unconstrained locomotion," *Biomed. Signal Process. Control*, vol. 60, Jul. 2020, Art. no. 101968.
[15] J. Liu, S. H. Kang, D. Xu, Y. Ren, S. J. Lee, and L.-Q. Zhang, "EMG-based continuous and simultaneous estimation of arm kinematics in able-bodied individuals and stroke survivors," *Frontiers Neurosci.*, vol. 11, p. 480, Aug. 2017.
[16] R. Raj, R. Ramakrishna, and K. S. Sivanandan, "A real time surface electromyography signal driven prosthetic hand model using PID controlled DC motor," *Biomed. Eng. Lett.*, vol. 6, no. 4, pp. 276–286, Nov. 2016.
[17] U. J. Naeem and C. Xiong, "Neural-genetic model for muscle force estimationbased on EMG signal," *Commun. Inf. Sci. Manage. Eng.*, vol. 3, no. 6, p. 301, 2013.
[18] S. Guo, M. Pang, B. Gao, H. Hirata, and H. Ishihara, "Comparison of sEMG-based feature extraction and motion classification methods for upper-limb movement," *Sensors*, vol. 15, no. 4, pp. 9022–9038, Apr. 2015.
[19] F. E. Zajac, "Muscle and tendon: Properties, models, scaling, and application to biomechanics and motor control," *Crit. Rev. Biomed. Eng.*, vol. 17, no. 4, pp. 359–411, 1989.
[20] H. Milner-Brown, R. B. Stein, and R. Yemm, "Changes in firing rate of human motor units during linearly changing voluntary contractions," *J. Physiol.*, vol. 230, no. 2, p. 371, 1973.
[21] D. G. Lloyd and T. F. Besier, "An EMG-driven musculoskeletal model to estimate muscle forces and knee joint moments *in vivo*," *J. Biomech.*, vol. 36, no. 6, pp. 765–776, Jun. 2003.
[22] T. S. Buchanan, D. G. Lloyd, K. Manal, and T. F. Besier, "Neuromusculoskeletal modeling: Estimation of muscle forces and joint moments and movements from measurements of neural command," *J. Appl. Biomech.*, vol. 20, no. 4, pp. 367–395, Nov. 2004.
[23] J. Woods and B. Bigland-Ritchie, "Linear and non-linear surface emg/force relationships in human muscles. an anatomical/functional argument for the existence of both," *Amer. J. Phys. Med.*, vol. 62, no. 6, pp. 287–299, 1983.
[24] I. J. Leontaritis and S. A. Billings, "Input-output parametric models for non-linear systems part I: Deterministic non-linear systems," *Int. J. Control*, vol. 41, no. 2, pp. 303–328, Feb. 1985.
[25] I. J. Leontaritis and S. A. Billings, "Input-output parametric models for non-linear systems part II: Stochastic non-linear systems," *Int. J. Control*, vol. 41, no. 2, pp. 329–344, Feb. 1985.
[26] K. Worden, C. Surace, and W. Becker, "Uncertainty bounds on higher-order FRFs from Gaussian process NARX models," *Procedia Eng.*, vol. 199, pp. 1994–2000, Jan. 2017.
[27] Y. Li, J. Chen, L. Jiang, N. Zeng, H. Jiang, and M. Du, "The p53–Mdm2 regulation relationship under different radiation doses based on the continuous–discrete extended Kalman filter algorithm," *Neurocomputing*, vol. 273, pp. 230–236, Jan. 2018.
[28] S. Babak, *Biostatistics With R: An Introduction to Statistics Through Biological Data*. New York, NY, USA: Springer, 2012.
[29] M. R. Tucker, J. Olivier, A. Pagel, H. Bleuler, M. Bouri, O. Lambercy, J. R. del Millán, R. Riener, H. Vallery, and R. Gassert, "Control strategies for active lower extremity prosthetics and orthotics: A review," *J. Neuroeng. Rehabil.*, vol. 12, no. 1, p. 1, 2015.
[30] R. Gupta and R. Agarwal, "Single channel EMG-based continuous terrain identification with simple classifier for lower limb prosthesis," *Biocybern. Biomed. Eng.*, vol. 39, no. 3, pp. 775–788, Jul. 2019.
[31] F. Di Nardo, C. Morbidoni, A. Cucchiarelli, and S. Fioretti, "Recognition of gait phases with a single knee electrogoniometer: A deep learning approach," *Electronics*, vol. 9, no. 2, p. 355, Feb. 2020.
[32] L. Sun, H. An, H. Ma, and J. Gao, "Real-time human intention recognition of multi-joints based on MYO," *IEEE Access*, vol. 8, pp. 4235–4243, 2020.
[33] Q. Ding, J. Han, and X. Zhao, "Continuous estimation of human multi-joint angles from sEMG using a state-space model," *IEEE Trans. Neural Syst. Rehabil. Eng.*, vol. 25, no. 9, pp. 1518–1528, Sep. 2017.

YURONG LI received the master's degree in industry automation and the Ph.D. degree in control theory and control engineering from Zhejiang University, in 1997 and 2001, respectively. Since 2007, she has been a member with the Fujian Key Laboratory of Medical Instrumentation and Pharmaceutical Technology. She is currently a Professor with Fuzhou University. Her research interests include biomedical instrument and intelligent information processing.

WENXIN CHEN received the B.E. degree in automation from the College of Electrical Engineering and Automation, Fuzhou University, Fuzhou, China, in 2018, where he is currently pursuing the master's degree in control engineering. His research interests include computational neuroscience and intelligent information processing.

HAO YANG received the B.E. degree in automation from the College of Mechanical and Electrical Engineering, East China University of Technology, Nanchang, China, in 2018. He is currently pursuing the master's degree in control science and engineering with Fuzhou University, Fuzhou, China. His research interest includes brain–computer interface technology.

JIXIANG LI was born in Zhoukou, Henan, China, in 1990. He is currently pursuing the Ph.D. degree in electrical engineering with Fuzhou University, Fujian, China. His research interests include biocomputing, biomedical instrument, and intelligent information processing.

NAN ZHENG received the B.E. degree in automation from the College of Computer and Electronic Information, Guangdong University of Petrochemical Technology, Maoming, China, in 2019. He is currently pursuing the master's degree in control science and engineering with Fuzhou University. His research interests include pattern recognition and feature extraction of EMG signals.